ELSEVIER

Ceramics International 32 (2006) 617–621

CERAMICS INTERNATIONAL

www.elsevier.com/locate/ceramint

Low temperature synthesis of hydroxyapatite from $CaHPO_4{\cdot}2H_2O$ and $Ca(OH)_2$ based on effect of the spark plasma system (SPS)

Mamoru Omori [a,*], Takamasa Onoki [a], Toshiyuki Hashida [a], Akira Okubo [b], Yoshihiro Murakami [b]

[a] *Graduate School of Engineering, Tohoku University, Fracture and Reliability Research Institute, 6-6-11 Aoba, Aramaki, Aoba-ku, Sendai 980-8579, Japan*

[b] *Institute for Materials Research, Tohoku University, 2-1-1 Katahira, Aoba-ku, Sendai 980-8577, Japan*

Received 28 November 2004; received in revised form 8 December 2004; accepted 23 April 2005
Available online 29 June 2005

Abstract

A mixture of 6 mol of $CaHPO_4{\cdot}2H_2O$ and 4 mol of $Ca(OH)_2$ was reacted to produce hydroxyapatite (HA) by spark plasma system (SPS). The reaction was carried out at 300–1200 °C under pressure of 20–670 MPa for 10 min in a vacuum. HA formation started at 300 °C at 600 MPa and was completed at 500 °C at 670 MPa, the same product being obtained at 1200 °C in air using a furnace. The temperature of the HA formation increased with decreasing pressure and was 1150 °C under 20 MPa. There was a linear relationship between the reaction temperature and pressure. The crystal size of the HA prepared at 500 °C at 670 MPa and that at 600 °C at 600 MPa by SPS were less than 1 and 2 μm, respectively.

Keywords: Hydroxyapatite; Hydroxyapatite synthesis; Spark plasma system (SPS); Spark plasma sintering (SPS); Calcium phosphate

1. Introduction

Powder sintering has been based on sintering at atmospheric pressure or sintering under high pressure. Although these techniques have enabled the manufacture of various kinds of useful products from metal and ceramics, their limited effectiveness for the production of advanced materials has recently become apparent. The spark plasma system (SPS) was developed for sintering metal and ceramic powders in plasma as well as in an electric field [1]. SPS is characterized by a pulsed direct electric current, which is similar to that of an electric discharge machine. Unique products which cannot be made by ordinary methods have been created from ceramics, metals and polymers by SPS [2]. The formation of these products is based on the effect of the pulsed electric field, where spark plasma is generated between powders and a skin current can run on particle surface. The spark plasma activates some chemical bonds, and crystal growth is enhanced by the skin current [2]. The mobility of dislocations is accelerated in the pulsed direct electric field [3].

Hydroxyapatite (HA, $Ca_{10}(PO_4)_6(OH)_2$) is one of the most bioactive ceramics [4]. The chemical composition of HA consists of OH groups which are eliminated at high temperature. The stability of HA depends on the partial pressure of H_2O [5]. The HA powder can be stably sintered at 1300 °C in air using a furnace [6]. On the other hand, HA is stable below 1050 °C in a vacuum [7]. The decomposition temperature of HA is lowered till 800 °C by the catalytic action of Ti [8,9]. The majority of HA syntheses are carried out under the influence of water as follows: (1) precipitation method [10,11]; (2) hydrolysis method [12]; (3) hydrothermal method [13,14]; and (4) hydrothermal hot-pressing method [15]. HA is synthesized from 6 mol of $CaHPO_4$ (DCP) and 4 mol of $Ca(OH)_2$ (CHO) without water by solid state reaction [4], although the synthetic condition has not been clarified.

* Corresponding author. Tel.: +81 22 217 7524; fax: +81 22 217 4311.
E-mail address: m-omori@rift.mech.tohoku.ac.jp (M. Omori).

0272-8842/$30.00
doi:10.1016/j.ceramint.2005.04.021

In this study, 6 mol of $CaHPO_4{\cdot}2H_2O$ (DCPD) and 4 mol of CHO were reacted to produce hydroxyapatite by SPS. The reaction was carried out at 300–1200 °C under pressure of 20–670 MPa. The HA formation was investigated by X-ray diffractometry, and the grain size of the prepared HA was observed by scanning electron microscopy (SEM) and transmission electron microscopy (TEM).

2. Experimental

2.1. Materials and reaction

The starting powders were DCPD and CHO (Wako Pure Chemical Ind., Japan, reagent grade), 6 mol of DCPD and 4 mol of CHO being mixed with an agate mortar and pestled for 20 min. These two materials were reacted by SPS (Sumitomo Coal Mining Co. Ltd., Japan, SPS1050). The mixed powder was put in a graphite die or a hard metal die and heated from 300 to 1200 °C at 20–670 MPa in a vacuum. The heating rate was controlled toward the goal temperature of 1000 °C as follows: from 20 to 900 °C at 100 °C/min, from 900 to 980 °C at 20 °C/min and from 980 to 1000 °C at 5 °C/min. The holding time at the goal temperatures was 10 min. For comparison with the SPS sample, the mixed powder was reacted from 500 to 1200 °C in air in a furnace without using SPS.

2.2. Decomposition of materials and characterization of the reacted product

The decomposition temperature of DCPD was determined by differential scanning calorimetry at a heating rate of 0.67 °C/s in air (Seiko Instruments, Japan, SII DSC 6300). The reacted products were subjected to X-ray diffraction (XRD) by an X-ray diffractometer (Rigaku, Japan, Rotaflex, RU-200B) using the Cu Kα line. The surface of the reacted product was polished to make a mirror surface and was etched at 1000 °C for 30 min in air. The etched surface of the sintered product was observed by a scanning electron microscope (SEM) (JEOL, Japan, JXA-8621MX, and Hitachi, Japan, S-800). The microstructure was analyzed by a transmission electron microscope (TEM) (JEOL, Japan, JT-007).

3. Results

3.1. Reaction in furnace

The results of the DSC measurement indicated that DCPD lost water and was transformed into DCP at 149 °C. DCP was decomposed at 460 °C. It was confirmed by X-ray diffractometry that CHO was stable until 900 °C and then decomposed into CaO over 1000 °C. The mixture of 6 mol of DCP and 4 mol of CHO was reacted in air in a furnace, not using SPS. The reaction of DCPD and CHO did not occur at 500 °C, but started near 600 °C. Fig. 1a shows that HA with impurities was formed at 600 °C for 1 h. The diffraction peaks of the product was not sharp and exhibited the formation of a small crystallite, i.e. nucleus. This nucleus was unstable at this temperature and disappeared after heating at 600 °C for 10 h. The nucleus did not grow to stable size at 600 °C in the furnace.

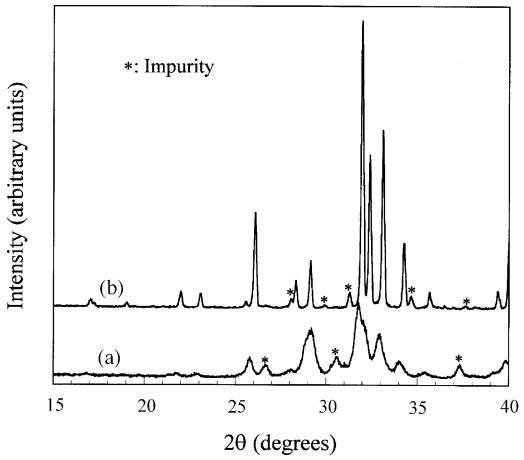

Fig. 1. XRD patterns of the products reacted in furnace for 1 h in air: (a) at 600 °C and (b) at 1200 °C.

The formation of HA from DCP and CHO was indistinct below 1000 °C, but was distinguishable at 1200 °C. The reacted product consisted of HA and a small amount of the impurity which was not identified, as shown in Fig. 1b. It was clear that preparation of HA was possible in air by solid state reaction. Judging from the half-value width of the diffraction peaks, the crystal of the product which prepared at 1200 °C was not a nucleus, The HA crystal was stable and did not decompose after the reaction at 1200 °C for 10 h in air. The impurity neither decreased nor increased after the long reaction.

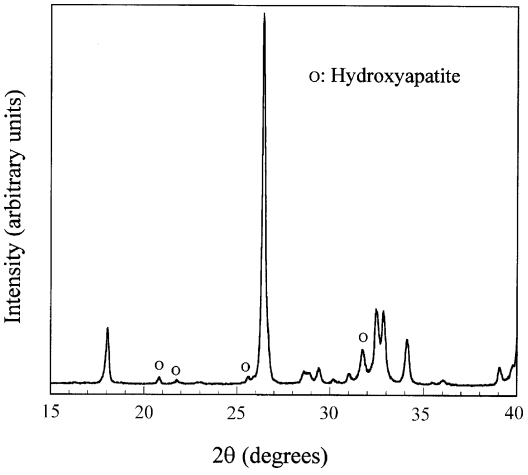

Fig. 2. XRD pattern of the product reacted at 300 °C at 600 MPa for 10 min by SPS.

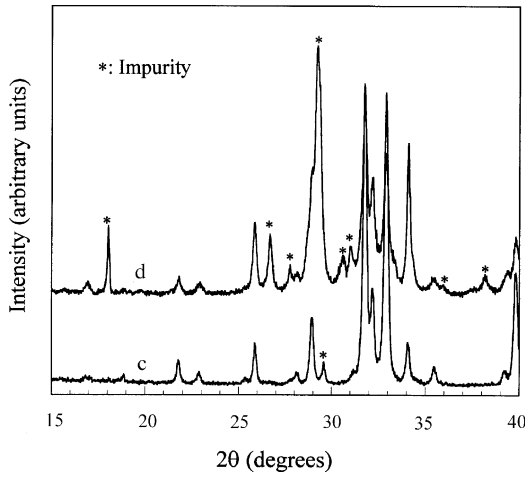

Fig. 3. XRD patterns of the products reacted at 500 °C for 10 min by SPS: (c) at 670 MPa and (d) at 20 MPa.

3.2. Reaction by SPS

The reaction by SPS was different from that conducted in air using a furnace. The X-ray diffraction pattern shown in Fig. 2 suggests that DCP and CHO started reacting at 300 °C under high pressures. This reaction occurred at 600 MPa, but it was not completed within 1 h. The low pressure of 20 MPa did not induce the reaction between these two compounds. The HA formation was clear for the product reacted at 500 °C at 670 MPa for 10 min. This product was composed of HA and a small amount of impurities, as shown in Fig. 3c. The impurities were not identified. The X-ray diffraction pattern shown in Fig. 3d indicates that the impurities increased at 20 MPa. SPS enabled production of HA at 500 °C, despite under the high pressure. The HA formation temperature increased with decreasing pressure.

Fig. 4e shows that the product reacted at 600 °C at 600 MPa was the nearly same as that prepared at 500 °C. The impurity was not removed after the reaction at 500 and 600 °C for 1 h and persisted in the product. A pure HA product was obtained by the reaction at 700 °C at 470 MPa for 10 min, as shown in Fig. 4f. The crystals of those products were stable and different from the nucleus synthesized at 600 °C in the furnace. HA was prepared at 1000 °C at 120 MPa and at 1150 °C at 20 MPa. X-ray diffraction pattern of the products reacted at these two temperatures is shown in Fig. 4g and h. The reacted product contained unidentified impurities. The impurities remained in the product reacted at 1200 °C at 20 MPa.

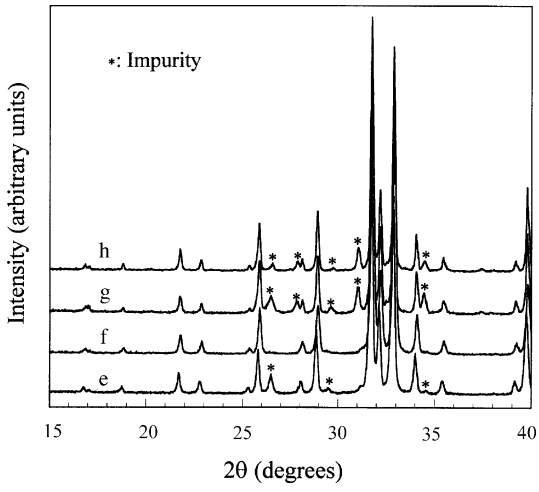

Fig. 4. XRD patterns of the products reacted for 10 min by SPS: (e) at 600 °C at 600 MPa; (f) at 700 °C at 480 MPa; (g) at 1000 °C at 120 MPa and (h) at 1150 °C at 20 MPa.

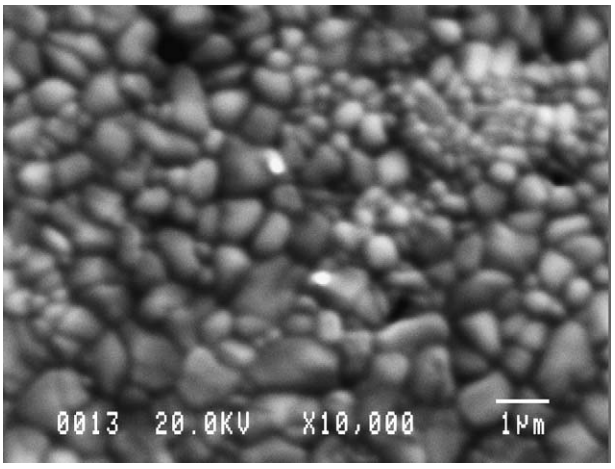

Fig. 5. SEM image of the product reacted at 500 °C at 670 MPa for 10 min by SPS.

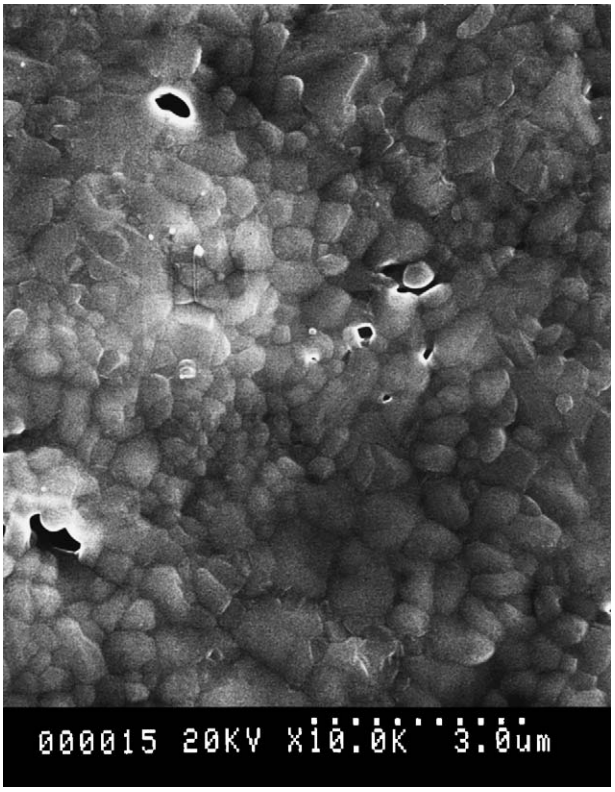

Fig. 6. SEM image of the product reacted at 600 °C at 600 MPa for 10 min by SPS.

The diffraction peaks were broadened in the products reacted at 500 °C compared with those of the products prepared at 1200 °C in the furnace and from 600 to 1150 °C by SPS. This broadening suggested that the crystal size of the product was small or that the crystallinity was not good.

The crystal size was measured on the etched surface of the product reacted at 500 °C at 670 MPa for 10 min. The SEM image shown in Fig. 5 indicates the crystal size to be less than 1 μm. Fig. 6 shows that the crystal size of the product reacted at 600 °C at 600 MPa was less than 2 μm. TEM observation of the HA crystal reacted at 1150 °C at 20 MPa for 10 min revealed its size to be less than 2 μm. The crystal size of the products reacted from 500 to 1150 °C was not greatly affected by the reaction temperature.

4. Discussion

DCPD lost water of crystallization at 149 °C and became to DCP. The real reaction of DCPD and CHO is that of DCP and CHO over this temperature. The reaction of these two compounds starts at 600 °C in the furnace after decomposition of DCP, and HA nuclei with impurities are produced. The nucleus is unstable and decomposed without water. Time is required for the nucleus to change into a stable crystal at the low temperature when using the furnace. The water supply based on the decomposition of the two compounds cannot last for a long time, and the nucleus is transformed into other stable compounds different from HA. The product reacted at 1200 °C for 1 h in the furnace contained the impurity, and its amount did not increase nor decrease by the long reaction for 10 h. This impurity is not derived from decomposition of the formed HA because β-$Ca_3(PO_4)_2$ is not included, but it is produced in the course of the reaction of DCP and CHO.

The Ca/P ratio of hydroxyapatite is not constant and varies from 1.65 to 1.72 [16]. The product fabricated from the mixture of 6 mol of DCPD and 4 mol of CHO must result in the composition of 1.67, and the one reacted at 700 °C at 480 MPa corresponds it not accompanied by the impurity. The impurity in other products suggests that the composition of the product differs from that of the mixture. There was an impurity peak at $2\theta = 29.6°$ in the XRD pattern shown in Fig. 3c. The mixture was synthesized from 3.9 to 4.1 mol of CHO for 6 mol of DCPD and reacted at 500 °C at 670 MPa to eliminate this impurity. The XRD patterns shown in Fig. 7i and j, which were obtained from the inside and surface of the same product pellet, were due to the product synthesized from 6 mol of DCPD and 3.93 mol of CHO (Ca/P = 1.66). The intensity of the impurity peaks was the least among the products reacted in that composition variation. As shown in Fig. 7i, that impurity peak at $2\theta = 26.9°$ was removed, and new weak ones appeared at $2\theta = 20.4°$, 26.6°, 31.2° and 34.5°. The feature of the impurity peaks indicated in Fig. 7j was not same as that of the inside and revealed that the Ca/P ratio varied from the surface to the inside. The impurity does not mean that the reaction is not completed at each temperature and pressure.

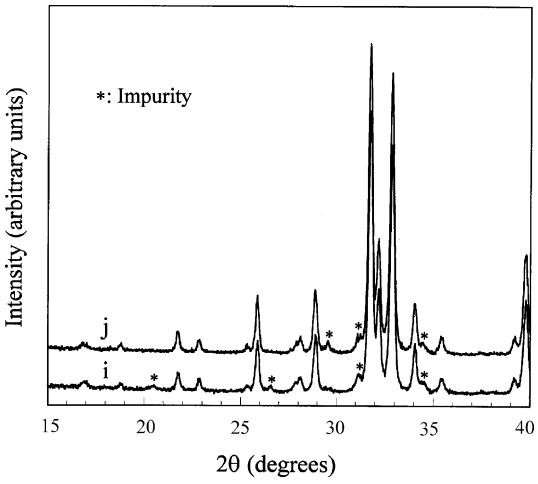

Fig. 7. XRD patterns of the products reacted from 6 mol of DCPD and 3.93 mol of CHO at 500 °C at 670 MPa for 10 min by SPS and measured: (i) at the inside and (j) at the surface.

SPS can enhance the reaction of DCP and CHO, and HA is produced at lower temperatures under higher pressures. The reaction by SPS is different from that in the furnace. DCP was not damaged at 20 and 670 MPa at 300 °C by SPS. On the other hand, CHO was slightly decomposed at 20 and 670 MPa at 300 °C. The reaction of DCP and CHO is initiated at 300 °C by degradation of CHO. High pressure enhances the reaction, and HA is formed at 500 °C under the pressure of 670 MPa, which is near the endurance limit of hard metal. The product reacted at 500, 600, 1000 and 1150 °C consists of HA and small portions of impurities, and they comes from the excess DCP or CHO. There is a liner relationship between the reaction temperature and pressure, as shown in Fig. 8. The high pressure causes the isolated particles to come into tight contact. Furthermore, since mobility of dislocations is enhanced in the pulsed electric field [3], it is possible that the compound particles are plastically deformed at lower temperatures. The contact area (or necking area) is effectively widened under high pressure by plastic deformation. The

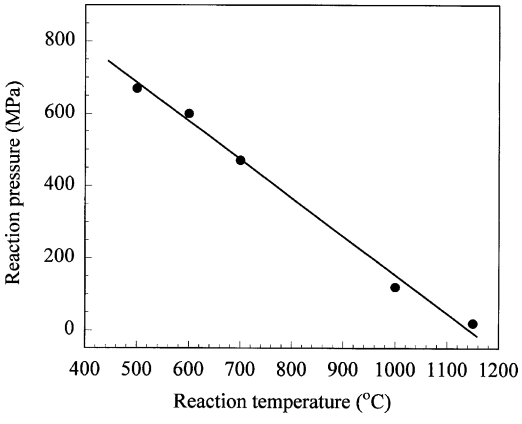

Fig. 8. Temperature vs. pressure for HA formation by SPS.

molecules of the two compounds can diffuse through the wide contact area.

One of the SPS effects is based on the skin current, which appears on the surface of particles in the pulsed electric field and results in acceleration of crystal growth [2]. If the skin current is determined by the voltage applied to the graphite die, its density varies with the free surface of particles excluding the contact area. The volume of the free surface decreases at high pressure because of the increased contact area. The migration of Al atoms in the Al film is accelerated through direct current [17], but there is no evidence regarding the accelerated migration of molecules in the pulsed direct electric field. The skin current may carry the DCP and CHO molecules on the surface of the particles. The wide contact area and the enhanced migration enable the reaction at the low temperatures and result in the linear relationship between the reaction temperature and pressure.

The half-value width of the X-ray diffraction peak suggests that the crystal size of the product reacted at 500 °C is less than that of the ones synthesized from 600 to 1150 °C. However, the size observed by SEM and TEM is almost same, i.e. less than 1 and 2 μm. The crystals prepared at 500 °C contain many of crystal imperfections, such as lattice defects and stacking faults, and the diffraction peaks are broadened by them. The crystal size of the products reacted at 600 and 1150 °C is not different. This result is contrary to the fact that growth rate of crystal is faster at higher temperature. HA molecules can be carried on the surface of the HA crystal under higher pressures by the dense skin current, and the crystal growth is promoted by it.

5. Conclusion

$CaHPO_4{\cdot}2H_2O$ (6 mol) and $Ca(OH)_2$ (4 mol) were reacted at 1200 °C for 1 h in air using a furnace and produced HA. Using the spark plasma system, HA formation started at 300 °C at 600 MPa and was completed at 500 °C at 670 MPa for 10 min. The temperature of the HA formation increased with decreasing pressure. HA was prepared for 10 min at 600 °C, 700, 1000 and 1150 °C under pressures of 600, 470, 120 and 20 MPa, respectively. There was a linear relationship between the temperature and pressure of the SPS reaction. The effects of SPS, namely, the plastic deformation enhanced in the pulsed electric field and the skin current generated on particle surface in an electric field, enabled the reaction of the two compounds at lower temperatures under higher pressures. The size of the HA crystal reacted at 500 °C at 670 MPa was similar to that of the one formed at 1150 °C at 20 MPa. The skin current under the high pressure was responsible for the crystal growth of HA at the low temperatures.

Acknowledgements

This study was supported by Research on Advanced Medical Technology in Health and Labour Sciences Research Grants from the Ministry of Health, Labour and Welfare of Japan. The authors are thankful to Mr. Shun Ito (Institute for Materials Research, Tohoku University) for transmission electron microscope, observations.

References

[1] K. Inoue, Electric-discharge sintering. US Patent No. 3,241,956 (1966).
[2] M. Omori, Sintering, consolidation, reaction and crystal growth by the spark plasma system (SPS), Mater. Sci. Eng. A287 (2000) 183–188.
[3] H. Conrad, Electroplasticity in metals and ceramics, Mater. Sci. Eng. A287 (2000) 276–287.
[4] R.Z. Legeros, J.P. Legeros, Dense hydroxyapatite, in: L.L. Hench, J. Wilson (Eds.), Advanced Series in Ceramics: Introduction to Bioceramics, vol. 1, World Scientific, NJ, USA, 1991, pp. 139–180.
[5] P.V. Ribound, Comparaison de la stabilite de l'apatite d'oxyde de fer et de l'hydroxyapatite a haute temperature, Bull. Soc. Chim. Fr. (1968) 1701–1703.
[6] P. Van Landuyt, F. Li, J.P. Keustermans, J.M. Streydio, F. Delannay, E. Munting, The influence of high sintering temperatures on the mechanical properties of hydroxyapatite, J. Mater. Sci.: Mater. Med. 6 (1995) 8–13.
[7] J.C. Trombe, G. Montel, Some features of the incorporation of oxygen in different oxidation states in the apatitic lattice. I. On the existence of calcium and strontium oxyapatites, J. Inorg. Nucl. Chem. 40 (1978) 15–21.
[8] P. Ducheyne, S. Radin, M. Heughebaert, J.C. Heughebaert, Calcium phosphate ceramic coatings on porous titanium: effect of structure and composition on electrophoretic deposition, vacuum sintering and in vitro dissolution, Biomaterials 11 (1990) 244–254.
[9] J. Weng, X. Liu, X. Zhang, X. Ji, Thermal decomposition of hydroxyapatite structure induced by titanium and its dioxide, J. Mater. Sci. Lett. 13 (1994) 159–161.
[10] W. Rathje, Zur Kenntnis der Phosphate. I. Uber Hydroxyapatite, Bodenk. Pflernach. 12 (1939) 121–128.
[11] E. Hayek, H. Newsely, Pentacalcium monohydroxyorthophosphate (hydroxyapatite), Inorg. Synth. 7 (1963) 63–65.
[12] H. Monma, T. Kamiya, Preparation of hydroxyapatite by the hydrolysis of brushite, J. Mater. Sci. 22 (1987) 4247–4250.
[13] E. Hayer, J. Lechleitner, W. Bohler, Hydrothermalsynthese von hydroxyapatite, Angew. Chim. 67 (1955) 326.
[14] O.R. Trautz, X-ray diffraction of biological and synthetic apatites, Ann. N. Y. Acad. Sci. 60 (1955) 696–712.
[15] K. Hosoi, T. Hashida, H. Tkahashi, N. Yamasaki, T. Korenaga, New processing technique for hydroxyapatite ceramics by the hydrothermal hot-pressing method, J. Am. Ceram. Soc. 79 (1996) 2771–2774.
[16] M. Jarcho, C.H. Bolen, M.B. Thomas, J. Bobick, J.F. Kay, R.H. Doremus, Hydroxyapatite synthesis and characterization in dense polycrystalline form, J. Mater. Sci. 11 (1976) 2027–2035.
[17] I.A. Blench, Electromigration in thin aluminum films on titanium nitride, J. Appl. Phys. 47 (1976) 1203–1208.